Hydrol. Earth Syst. Sci. Discuss., doi:10.5194/hess-2016-295, 2016
Manuscript under review for journal Hydrol. Earth Syst. Sci.
Published: 20 June 2016

Hydrology and Earth System Sciences
Open Access
Discussions

Hydraulic and transport parameter assessment using column infiltration experiments

A. Younes[1,2,3], T.A. Mara[4], M. Fahs[1], O. Grunberger[2], Ph. Ackerer[*,1]

[1] LHyGES, Université de Strasbourg/EOST, CNRS, 1 rue Blessig, 67084 Strasbourg, France.
[2] IRD UMR LISAH, F-92761 Montpellier, France.
[3] LMHE, Ecole Nationale d'Ingénieurs de Tunis, Tunisie
[3] Université de La Réunion, PIMENT, 15 Avenue René Cassin, BP 7151, 97715 Moufia, La Réunion.

Submitted to

* Contact person: Ph. Ackerer
E-mail: ackerer@unistra.fr

Hydrol. Earth Syst. Sci. Discuss., doi:10.5194/hess-2016-295, 2016
Manuscript under review for journal Hydrol. Earth Syst. Sci.
Published: 20 June 2016

Hydrology and Earth System Sciences
Discussions
Open Access

Abstract

In the present work, we study the quality of the statistical calibration of hydraulic and transport soil properties using an infiltration experiment in which, over a given period, tracer-contaminated water is injected into a laboratory column filled with a homogeneous soil. The numerical model is based on the Richards' equation for solving water flow and the advection-dispersion equation for solving solute transport. Several state variables (e.g., water content, solute concentration, pressure head) are measured during the experiment. Statistical calibration of the computer model is then carried out for different data sets and injection scenarios with the $\mathrm{DREAM}_{(\mathrm{ZS})}$ Markov Chain Monte Carlo sampler. The results show that the injection period has a significant effect on the quality of the estimation, in particular, the posterior uncertainty range. The hydraulic and transport parameters of the investigated soil can be estimated from the infiltration experiment using the concentration and cumulative outflow, which are measured non-intrusively. A significant improvement of the identifiability of the parameters is observed when the pressure data from measurements taken inside the column are also considered in the inversion.

Keywords

Infiltration experiment, Richards' equation, Statistical calibration, Markov Chain Monte Carlo, Uncertainty ranges.

1. Introduction

The soil parameters that influence water flow and contaminant transport in unsaturated zones are not generally known *a priori* and have to be estimated by fitting model responses to observed data. Several studies have demonstrated that unsaturated soil hydraulic parameters can be (more or less accurately) estimated from dynamic flow experiments (*e.g.*, Hopmans et al., 2002; Vrugt et al., 2003a; Durner and Iden, 2011; Younes et al., 2013). Inoue et al. (2000) showed that both hydraulic and transport parameters can be assessed by the combination of flow and transport experiments. Indeed, the simultaneous estimation of hydraulic and transport properties yields smaller estimation errors for model parameters than the sequential inversion of hydraulic properties from the water content and/or pressure head followed by the inversion of transport properties from concentration data (Misra and Parker, 1989).

In the present work, we consider the flow and the transport of an inert solute injected into a laboratory column filled with a homogeneous sandy clay loam soil. The flow-transport model is described by the Richards' equation (RE) for water flow and the advection dispersion equation for solute transport. The Mualem-van Genuchten (MvG) models (Mualem 1976, van Genuchten 1980) are chosen to describe the retention curve and to relate the hydraulic conductivity of the unsaturated soil to the water content. The estimation of hydraulic and transport parameters is performed in a Bayesian framework using the Markov Chain Monte Carlo (MCMC) sampler (Vrugt and Bouten, 2002; Vrugt et al., 2008) for two injection periods and different data measurement scenarios. Unlike classical parameter optimization algorithms, the MCMC approach provides parameter joint probability distributions, which are useful for the quality assessment of the estimation. Indeed, MCMC samples can be used to summarize parameter uncertainties and to perform predictive uncertainty (Ades and Lu, 2003).

Hydrol. Earth Syst. Sci. Discuss., doi:10.5194/hess-2016-295, 2016
Manuscript under review for journal Hydrol. Earth Syst. Sci.
Published: 20 June 2016

Soil parameters are usually investigated using multistep outflow experiments (e.g., Eching and Hopmans, 1993; Eching et al., 1994; van Dam et al., 1994) or continuously changing time-varying boundary conditions (Durner et al., 1999). Multistep outflow experiments are among the most popular laboratory methods (Hopmans et al., 2002). However, their application is limited by expensive measurement equipment (Nasta et al., 2011).

In this work, hydraulic soil parameters are investigated using an infiltration experiment in a 1.2 m long laboratory column, which is the standard scale for these types of experiments. The column, which is initially hydrostatic and free of solute, is filled with a homogeneous sandy clay loam soil. Continuous flow and solute injection are performed during a time period T_{inj} at the top of the column and with a zero pressure head at the bottom. The unknown parameters for the water flow are k_s [LT^{-1}], the saturated hydraulic conductivity; θ_s [L^3L^{-3}], the saturated water content; θ_r [L^3L^{-3}], the residual water content; and α [L^{-1}] and n [−], the MvG shape parameters. The only unknown parameter of the tracer transport is the longitudinal dispersivity, a_L [L].

Several scenarios corresponding to different sets of measurements are investigated to address the following questions:

1) Can we obtain an appropriate estimation of all flow and transport parameters from the tracer-infiltration experiment, even though only moderately dry conditions are used?
2) What is the optimal set of measurements for the estimation of all the parameters? Can we use only non-intrusive measurements (cumulative outflow and concentration breakthrough curve) or are intrusive measurements required, such as the analysis of the pressure head and/or water content inside the column?
3) Does the duration of the injection period T_{inj} have an impact on the identification of the parameters?

Hydrol. Earth Syst. Sci. Discuss., doi:10.5194/hess-2016-295, 2016
Manuscript under review for journal Hydrol. Earth Syst. Sci.
Published: 20 June 2016

Hydrology and Earth System Sciences
Open Access
Discussions

Synthetic scenarios are considered in the sequel in which data from numerical simulations are manipulated to avoid the uncontrolled noise of experiments that could bias the conclusions.

The paper is organized as follows. The mathematical models describing flow and transport in the unsaturated zone are detailed in section 2. Section 3 describes the MCMC Bayesian parameter estimation procedure used in the DREAM$_{(ZS)}$ sampler. Section 4 presents the different investigated scenarios and discusses the results of the calibration in terms of mean parameter values and uncertainty ranges for each scenario. Conclusions are given in section 5.

2. Unsaturated flow-transport model

We consider a uniform soil profile in the column and an injection of a solute tracer such as bromide, as described in Mertens et al. (2009). The unsaturated water flow in the vertical soil column is modeled with the one-dimensional pressure head form of the RE:

$$\begin{cases} \left(c(h)+S_s\dfrac{\theta}{\theta_S}\right)\dfrac{\partial h}{\partial t}=\dfrac{\partial q}{\partial z} \\ q=K(h)\left(\dfrac{\partial h}{\partial z}-1\right) \end{cases}, \tag{1}$$

where h [L] is the pressure head; q [LT^{-1}] is the Darcy velocity; z [L] is the depth, measured as positive in the downward direction; S_s (-) is the specific storage; θ and θ_s [L^3.L^{-3}] are the actual and saturated water contents, respectively; $c(h)$ [L^{-1}] is the specific moisture capacity; and $K(h)$[L T^{-1}] is the hydraulic conductivity. The latter two parameters are both functions of the pressure head. In this study, the relations between the pressure head, conductivity and water content are described by the following standard models of Mualem (1972) and van Genuchten (1980):

Hydrol. Earth Syst. Sci. Discuss., doi:10.5194/hess-2016-295, 2016
Manuscript under review for journal Hydrol. Earth Syst. Sci.
Published: 20 June 2016

$$S_e(h)=\frac{\theta(h)-\theta_r}{\theta_s-\theta_r}=\begin{cases}\dfrac{1}{\left(1+|\alpha h|^n\right)^m} & h<0\\ 1 & h\geq 0\end{cases} \tag{2}$$
$$K(S_e)=K_s S_e^{1/2}\left[1-\left(1-S_e^{1/m}\right)^m\right]^2 ,$$

where S_e (-) is the effective saturation, θ_r [$L^3\ L^{-3}$] is the residual water content, K_s [$L\ T^{-1}$] is the saturated hydraulic conductivity, and $m=1-1/n$, α [L^{-1}] and n (-) are the MvG shape parameters.

The tracer transport is governed by the following convection-dispersion equation:

$$\frac{\partial(\theta C)}{\partial t}+\frac{\partial(qC)}{\partial z}-\frac{\partial}{\partial z}\left(\theta D\frac{\partial C}{\partial z}\right)=0 , \tag{3}$$

where C [ML^{-3}] is the concentration of the tracer, D [$L^2\ T^{-1}$] is the dispersion coefficient in which $D=a_l\,q+d_m$ and a_l [L] is the dispersivity coefficient of the soil and d_m [$L^2\ T^{-1}$] is the molecular diffusion coefficient, which is set as 1.04 10^{-4} cm^2/min.

The initial conditions are as follows: a hydrostatic pressure distribution with zero pressure head at the bottom of the column $(z=L)$ and a solute concentration of zero inside the whole column. An infiltration with a flux q_{inj} of contaminated water with a concentration C_{inj} is then applied at the upper boundary condition (z = 0) during a period T_{inj}. Hence, the boundary conditions at the top of the column can be expressed as:

$$for\ 0<t\leq T_{inj}\begin{cases}K\left(\dfrac{\partial h}{\partial z}-1\right)=q_{inj}\\ \theta D\dfrac{\partial C}{\partial z}+qC=q_{inj}C_{inj}\end{cases}\qquad for\ t>T_{inj}\begin{cases}K\left(\dfrac{\partial h}{\partial z}-1\right)=0\\ C_{inj}=0\end{cases} \tag{4}$$

A zero pressure head is maintained at the lower boundary $(z=L)$ of the column and a zero concentration gradient is used as the lower boundary condition for the solute transport.

Hydrol. Earth Syst. Sci. Discuss., doi:10.5194/hess-2016-295, 2016
Manuscript under review for journal Hydrol. Earth Syst. Sci.
Published: 20 June 2016

$$(h)_{z=l} = 0 \qquad \left(\frac{\partial C}{\partial z}\right)_{z=l} = 0 \tag{5}$$

In the sequel, the infiltration rate and the injected solute concentration are $q_{inj} = 0.015$ cm/min and $C_{inj} = 1$ g/cm^3, respectively. The system (1)-(3) is solved using the finite volume method for both flow and transport spatial discretization. A uniform mesh of 600 cells is employed. Temporal discretization is performed with the high-order method of lines (MOL) (e.g., Miller et al., 1998; Tocci et al., 1997; Fahs et al., 2009). Error checking, robustness, order selection and adaptive time step features, available in sophisticated solvers, are applied to the time integration of partial differential equations in the MOL (Tocci et al., 1997). The MOL has been successfully used to solve RE in many studies (e.g., Farthing et al., 2003; Miller et al., 2006; Li et al., 2007; Fahs et al., 2009).

The unknown parameters for the water flow are k_s, θ_s, θ_r and the MvG shape parameters α and n. The only unknown parameter of the tracer transport is the longitudinal dispersivity a_L. Hence, the total vector of parameters is $\xi = (k_s, \theta_s, \theta_r, \alpha, n, a_L)$. A reference solution is generated using the following parameter values (corresponding to a sandy clay loam soil): $k_s = 50\,cm/day$, $\theta_s = 0.43$, $\theta_r = 0.09$, $\alpha = 0.04\,cm^{-1}$, $n = 1.4$ and $a_l = 0.2\,cm$. Four types of observations are deduced from the results of the simulation, which include the following: the pressure head and water content near the surface (5 cm below the top of the column) as well as the cumulative outflow and the breakthrough concentration at the output of the column. The vector of observations y_{mes} is formed by the four data series, which are independently corrupted with a normally distributed noise using the following standard deviations: $\sigma_h = 1cm$ for the pressure head, $\sigma_\theta = 0.02$ for the water content, $\sigma_Q = 0.1$cm for the cumulative outflow and $\sigma_C = 0.01$ g/cm^3 for the exit concentration.

3. Bayesian parameter estimation

The flow-transport model is used to analyze the effects of different measurement sets on parameter identification. For this purpose, we adopt a Bayesian approach that involves the parameter joint posterior distribution (Vrugt et al., 2008). The latter is assessed with the DREAM$_{(ZS)}$ MCMC sampler (Laloy and Vrugt, 2012). This software generates random sequences of parameter sets that asymptotically converge toward the target joint posterior distribution (Gelman et al., 1997). Thus, if the number of runs is sufficiently high, the generated samples can be used to estimate the statistical measures of the posterior distribution, such as the mean and variance among other measures.

The Bayes theorem states that the probability density function of the model parameters conditioned onto data can be expressed as:

$$p(\xi \mid \boldsymbol{y}_{mes}) \propto p(\boldsymbol{y}_{mes} \mid \xi)\, p(\xi), \qquad (6)$$

where $p(\xi \mid \boldsymbol{y}_{mes})$ is the likelihood function measuring how well the model fits the observations $\boldsymbol{y}_{mes}$, and $p(\xi)$ is the prior assumption of the parameter before the observations are made. In this work, a Gaussian distribution defines the likelihood function because the observations are simulated and corrupted with Gaussian errors. In addition, independent uniform priors are considered. Hence, the parameter posterior distribution is expressed as:

$$p(\xi \mid \boldsymbol{y}_{mes}) \propto exp\left(-\frac{SS_h(\xi)}{2\sigma_h^2}-\frac{SS_\theta(\xi)}{2\sigma_\theta^2}-\frac{SS_Q(\xi)}{2\sigma_Q^2}-\frac{SS_C(\xi)}{2\sigma_C^2}\right), \qquad (7)$$

where $SS_h(\xi)$, $SS_\theta(\xi)$, $SS_Q(\xi)$ and $SS_C(\xi)$ are the sums of the squared differences between the observed and modeled data of the pressure head, water content, cumulative outflow and output concentration, respectively. For instance, $SS_h(\xi)=\sum_{k=1}^{Nh}\left(h_{mes}^{(k)}-h_{mod}^{(k)}(\xi)\right)^2$, which includes the observed and predicted pressure heads $h_{mes}^{(k)}$ and $h_{mod}^{(k)}$ at time t_k and the number of pressure head observations Nh.

Bayesian parameter estimation is performed hereafter with the $DREAM_{(ZS)}$ software (Laloy and Vrugt, 2012), which is an efficient MCMC sampler. $DREAM_{(ZS)}$ computes multiple sub-chains in parallel to thoroughly explore the parameter space. Archives of the states of the sub-chains are also stored and used to allow a strong reduction of the "burn-in" period in which the sampler generates individuals with poor performances. Taking the last 25% of individuals of the MCMC (when the chains have converged) yields multiple sets of parameters, ξ, that adequately fit the model onto observations. These sets are then used to estimate the updated parameter distributions, the pairwise parameter correlations and the uncertainty of the model predictions. As suggested in Vrugt et al. (2003b), the posterior distribution becomes stationary if the Gelman and Ruban (1992) criterion is ≤ 1.2.

4. Results and discussion

In this section, the identifiability of the parameters is investigated for different scenarios of measurement sets and for two periods of injections. In all cases, the MCMC sampler was run with 3 simultaneous chains for a total number of 50000 runs. Depending on the scenario, the MCMC required between 5000 and 20000 model runs to reach convergence. The last 25% of the runs that adequately fit the model onto observations are used to estimate the updated probability density function (pdf).

4.1. Reference solution and data measurements

The reference solutions obtained from solving the flow-transport problems (1)-(3) using the parameters given above are shown in Fig. 1 to 6. The pressure head at 5 cm, at the top of the column (Fig. 1), increases quickly from its initial hydrostatic negative value (approximately -

115 cm) and reaches a plateau (-1.75 cm) during the injection period. After the injection is finished, it progressively decreases due to the drainage caused by the gravity effect. A similar behavior is observed for the water content at the same location (Fig. 2), where the value of the plateau is close to the saturation value. The cumulative outflow (Fig. 3) starts to increase at approximately 1000 min after the beginning of the injection. It shows an almost linear behavior until 5500 min. It then slowly increases with an asymptotic behavior due to the natural drainage after the end of the injection. Fig. 4 displays the water saturation as a function of the pressure head. It is worth noting that only a few parts of this curve are described during the infiltration experiment. Indeed, only moderate dry conditions are established because the minimum pressure head reached in the column is -120 cm, which corresponds to the initial pressure head near the top of the column.

The breakthrough concentration curve (Fig. 5) shows a sharp front, which starts shortly after 3000 min. If the injection of both water and contaminant are stopped once the solute reaches the output, i.e., after an injection period of 3000 min, the breakthrough curve exhibits a smoother progression (Fig. 6).

The observed data, which are used as conditioning information for model calibration, are also shown in Fig. 1to 6. Fig. 2 shows that the water content is more affected by the perturbation of data than by the pressure head and cumulative outflow because (*i*) we mimic the relative importance of the measurement errors of the water content due to time-domain-reflectometry probes and (*ii*) the weak variation of the water content during the infiltration experiment. The perturbation of the breakthrough curve is relatively small because output concentrations can be accurately measured. The perturbations of the pressure head and cumulative outflow seem weak because of the large variation of these variables during the experiment.

4.2. Results of the parameter estimation

The uncertainty model parameters are assumed to be distributed uniformly over the ranges reported in Table 1. This table also lists the reference values used to generate data observations before perturbation. Seven scenarios, corresponding to different sets of measurements for the estimation of the soil parameters, are considered (Table 2).

The MCMC results of the seven studied scenarios are given in Figs. 8 to 13. The "on-diagonal" plots in these figures display the inferred parameter distributions, whereas the "off-diagonal" plots represent the pairwise correlations in the MCMC sample. If the drawings are independent, non-sloping scatterplots should be observed. However, if a good value of a given parameter is conditioned by the value of another parameter, then their pairwise scatterplot should show a narrow sloping stripe. To facilitate the comparison between the different scenarios, Fig. 14 to 19 show the mean and the 95% confidence intervals of the final MCMC sample that adequately fit the model onto observations for each scenario, and Table 3 summarizes the pairwise parameter correlations.

Fig. 7 shows the inferred distributions of the parameters identified with the MCMC sampler using only the pressure and cumulative outflow measurements (scenario 1). The parameters k_s, α and n are well estimated; their prior intervals of variation are strongly narrowed and they essentially show bell-shaped posterior distributions. Parameter k_s is strongly correlated to α (0.94) and n (-0.97). Because the water retention relationship depends on the difference between θ_s and θ_r, these parameters are strongly correlated (0.96) and cannot be identified. The dispersivity coefficient a_l has not been identified.

The MCMC results (Fig. 8) show that θ_r strongly correlates to k_s (-0.94) and n (0.98) when water content measurements are added into the model (scenario 2). The parameter k_s remains strongly related to α (0.94) and n (-0.98). Although the water content data are subject to

Hydrol. Earth Syst. Sci. Discuss., doi:10.5194/hess-2016-295, 2016
Manuscript under review for journal Hydrol. Earth Syst. Sci.
Published: 20 June 2016

Hydrology and Earth System Sciences
Open Access
Discussions

relatively high measurement errors, a good estimation is obtained for θ_s and θ_r. The parameters k_s, α and n are estimated with the same accuracy as for the first scenario.

When the concentration measurements are also considered (scenario 3), the results depicted in Fig. 9 show very significant correlations between k_s and θ_r (-0.94), k_s and α (0.91), k_s and n (-0.97) and n and θ_r (0.99). The posterior uncertainty ranges of k_s, α, n and θ_r are similar to the previous scenarios. Those of θ_s and a_l are strongly reduced, leading to a good identification of these parameters when using C measurements (Fig. 15 and 19). A better estimate of the saturated water content is expected because advective transport is a function of this variable.

The measurements of the water content are not considered in the inversion procedure of scenario 4. This scenario leads to the same quality of the estimation for the parameters k_s, θ_r, α and n (Fig. 14, 16, 17, 18) and similar correlations between the parameters as in the previous scenario. This result shows that the intrusive water content measurements, which are subject to more measurement errors than the output concentration, are not required if the output concentration is measured. Compared with the results of scenario 2, it can be concluded that better parameter estimations are obtained using h, Q and C data than using h, Q and θ data, especially for θ_s. Therefore, using C instead of θ measurements in combination with h and Q measurements allows the estimation of a_l and leads to a better estimate of θ_s.

The pressure head, cumulative outflow and concentration measurements are used in the estimation procedure of scenario 5, but the injection period is now reduced to $T_{inj} = 3000\,\text{min}$. The obtained results (Fig. 11) show the same correlations between the parameters as for $T_{inj} = 5000\,\text{min}$. For the parameters k_s, θ_s, θ_r, α and n, almost the same mean estimates are obtained as for scenario 4. However, the parameters are better identified (Fig. 14 to 18). Indeed, the uncertainty of these parameters is smaller because the credible interval is reduced by a factor of 25% for k_s, 8% for θ_s, 26% for θ_r, 10% for α and 25% for n when compared to the results obtained for $T_{inj} = 5000\,\text{min}$. The parameter a_l is also estimated much better than in the previous scenario. Its mean value approaches the reference solution and the posterior uncertainty range is reduced by approximately 75% (Fig. 19).

The pressure head measurements are removed in scenario 6 and only non-intrusive measurements (Q and C data) are used with an injection period of $T_{inj} = 5000\,\text{min}$. The results depicted in Fig. 12 show high correlations only between k_s and n (-0.95) and θ_r and n (0.95). Compared with the results of scenario 4, which also considers the pressure data, k_s is poorly estimated (the mean value is less close to the reference value and the credible interval is 27% larger). The mean estimated values for θ_r and n also degraded (less close to the reference solution), although their confidence intervals are similar to those of scenario 4 (Fig. 16, 18). The estimated mean value of parameter α is similar to that in scenario 4. However, its uncertainty is much larger because the credible interval is 77% larger (Fig. 19). The parameters θ_s and a_l are estimated as well in scenario 4 (in terms of mean estimated value and credible interval).

The last scenario (scenario 7) is similar to the previous one, but the injection period is reduced to $T_{inj} = 3000\,\text{min}$. The results depicted in Fig. 13 show similar correlations between the parameters as for $T_{inj} = 5000\,\text{min}$. However, a significant improvement is observed for the mean estimated values, which approach the reference solution for k_s, θ_r, n and a_l (Fig. 14, 16, 18, 19). The uncertainties of k_s, α and a_l are also reduced by approximately 40%, 15% and 70%, respectively. The parameter θ_s is estimated as well in scenario 6.

5. Conclusions

In this work, hydraulic and transport soil parameters have been estimated using an infiltration experiment performed in a laboratory column filled with sandy clay loam soil, which was subjected to continuous flow and solute injection over a period T_{inj}. Parameter estimation was performed for different scenarios of data measurements in a Bayesian framework using the DREAM$_{(zs)}$ MCMC sampler (Laloy and Vrugt, 2012).

The results reveal the following conclusions:

1. All hydraulic and transport parameters can be appropriately estimated from the described infiltration experiment. However, the accuracy differs and depends on the type of measurement and the duration of the injection T_{inj}, even if the water content remains close to saturated conditions.
2. The use of concentration measurements at the column outflow, in addition to traditional measured variables (water content, pressure head and cumulative outflow), reduces the correlation between the hydraulic parameters and their uncertainties, especially that of the saturated water content.
3. The saturated hydraulic conductivity is estimated with the same order of accuracy, independent of the observed variables.
4. The estimation of the dispersivity is sensitive to the injection duration.
5. A better identifiability of the soil parameters is obtained using C instead of θ measurements, in combination with h and Q data.
6. Using only non-intrusive measurements (cumulative outflow and output concentration) allows the satisfactory estimation of all parameters. The uncertainty of the parameters significantly decreases when the injection of water and solute is maintained for a limited period.

Hydrol. Earth Syst. Sci. Discuss., doi:10.5194/hess-2016-295, 2016
Manuscript under review for journal Hydrol. Earth Syst. Sci.
Published: 20 June 2016

This last point has practical applications for designing simple experimental setups dedicated to the estimation of hydrodynamic and transport parameters for unsaturated flow in soils. The setup has to be appropriately equipped to measure the cumulative water outflow (e.g., weighing machine) and the solute breakthrough at the column outflow (e.g., flow through electrical conductivity). The injection should be stopped as soon as the solute concentration reaches the outflow. The accuracy of the estimation of θ_r, α and n can be improved by adding pressure measurements inside the column, close to the injection.

Acknowledgments

The authors are grateful to the French National Research Agency, which funded this work through the program AAP Blanc - SIMI 6 project RESAIN (n° ANR-12-BS06-0010-02).

Hydrol. Earth Syst. Sci. Discuss., doi:10.5194/hess-2016-295, 2016
Manuscript under review for journal Hydrol. Earth Syst. Sci.
Published: 20 June 2016

Hydrology and Earth System Sciences Discussions
Open Access

References

Ades A.E., G. Lu. 2003. Correlations between parameters in risk models: estimation and propagation of uncertainty by Markov Chain Monte Carlo. Risk Anal. 23(6):1165-72.

Durner W., B. Schultze, T. Zurmühl. 1999. State-of-the-art in inverse modeling of inflow/outflow experiments. p661-681. In M.Th. van Genuchten et al. (ed.) Characterization and Measurement of the Hydraulic Properties of Unsaturated Porous Media, Proc. Int. Worksh. Riverside, CA. Univ. of California, Riverside.

Durner W., S.C. Iden. 2011. Extended multistep outflow method for the accurate determination of soil hydraulic properties near water saturation. Water Resour. Res. 47:W08526. doi: 10.1029/2011WR010632

Eching S.O., J.W. Hopmans. 1993. Optimization of hydraulic functions from transient outflow and soil water pressure data. Soil Sci. Soc. Am. J. 57:1167-1175. doi:10.2136/sssaj1993.03615995005700050001x

Eching S.O., J.W. Hopmans, O. Wendroth. 1994. Unsaturated Hydraulic Conductivity from Transient Multistep Outflow and Soil Water Pressure Data. Soil Sci. Soc. Am. J. 58: 687-95 doi:10.2136/sssaj1994.03615995005800030008x

Fahs M., A. Younes, F. Lehmann. 2009. An easy and efficient combination of the Mixed Finite Element Method and the Method of Lines for the resolution of Richards' Equation. Environmental Modelling & Software ;24:1122–1126. doi:10.1016/j.envsoft.2009.02.010

Farthing M.W., Kees C.E., Miller C.T. 2003. Mixed finite element methods and higher order temporal approximations for variably saturated groundwater flow. Adv. in Water Resour. 26:373-394. doi: 10.1016/S0309-1708(02)00187-2

Inoue M., J. Šimůnek, S. Shiozawa, J.W. Hopmans. 2000. Simultaneous estimation of soil hydraulic and solute transport parameters from transient infiltration experiments, Adv. in Water Resour. 23 (7). Doi : 10.1016/S0309-1708(00)00011-7.

Haario H., E. Saksman, J. Tamminen. 2001. An adaptive Metropolis algorithm. Bernouilli, 3, 223-242.

Hopmans J.W., J. Simunek, N. Romano, W. Durner. 2002. Simultaneous determination of water transmission and retention properties. Inverse Methods. p963-1008. In J.H. Dane and G.C. Topp (ed.) Methods of Soil Analysis. Part 4. Physical Methods. Soil Science Society of America Book Series No. 5.

Gelman A., J.B. Carlin, H.S. Stren, D.B. Rubin. 1997. Bayesian data analysis, Chapmann and Hall, London.

Gelman A, D.B. Rubin. 1992. Inference from iterative simulation using multiple sequences. Stat. Sci. 7:457-472.

Laloy E., J.A. Vrugt. 2012. High-dimensional posterior exploration of hydrologic models using multiple-try DREAM(ZS) and high-performance computing, Water Resour. Res., 48, W01526. doi:10.1029/2011WR010608

Li H., M.W. Farthing, C.N. Dawson, C.T. Miller. 2007. Local discontinuous Galerkin approximations to Richards' equation. Adv. in Water Resour. 30:555–575. doi: 10.1016/j.advwatres.2006.04.011

Mertens J., G. Kahl, B. Gottesbüren, J. Vanderborght. 2009. Inverse Modeling of Pesticide Leaching in Lysimeters: Local versus Global and Sequential Single-Objective versus Multiobjective Approaches Vadose Zone J. 8(3). doi: 10.2136/vzj2008.0029

Miller CT, G.A. Williams, C.T. Kelly, M.D. Tocci. 1998. Robust solution of Richards' equation for non uniform porous media. Water Resour. Res. 34:2599–2610. doi: 10.1029/98WR01673

Miller C.T., C. Abhishek, M. Farthing. 2006. A spatially and temporally adaptive solution of Richards' equation. Adv. in Water Resour. 29:525–545. doi: 10.1016/j.advwatres.2005.06.008

Mishra S, J.C. Parker JC. 1989. Parameter estimation for coupled unsaturated flow and transport. Water Resour Res. 25(3). doi: 10.1029/WR025i003p00385

Mualem Y. 1976. A new model for predicting the hydraulic conductivity of unsaturated porous media. Water Resour. Res. 12:513–522. doi:10.1029/WR012i003p00513

Nasta P., S. Huynh, J.W. Hopmans. 2011. Simplified Multistep Outflow Method to Estimate Unsaturated Hydraulic Functions for Coarse-Textured Soil Sci. Soc. Am. J. 75, p.418. doi:10.2136/sssaj2010.011

Tocci MD, C.T. Kelly, C.T. Miller. 1997. Accurate and economical solution of the pressure-head form of Richards' equation by the method of lines. Adv. in Water Resour. 20:1–14. doi: 10.1016/S0309-1708(96)00008-5

van Dam J.C., J.N.M. Stricker, P. Droogers. 1994. Inverse method to determine soil hydraulic functions from multistep outflow experiments. Soil Sci. Soc. Am. J. 58:647-652. doi:10.2136/sssaj1994.03615995005800030002x

van Genuchten M.Th. 1980. A closed form equation for predicting the hydraulic conductivity of unsaturated soils. Soil Sci. Soc. Am. J. 44(5):892-898. doi:10.2136/sssaj1980.03615995004400050002x

Vrugt J.A., W. Bouten. 2002. Validity of first-order approximations to describe parameter uncertainty in soil hydrologic models. Soil. Sci. Soc. Am. J. 66:1740-1751. doi:10.2136/sssaj2002.1740

Vrugt J.A., W. Bouten, H.V. Gupta, J.W. Hopmans. 2003a. Toward improved identifiability of soil hydraulic parameters: On the selection of a suitable parametric model. Vadose Zone J. 2:98–113. doi: 10.2113/2.1.98

Vrugt J.A., H.V. Gupta, W. Bouten, S. Sorooshian. 2003b. A shuffled complex evolution Metropolis algorithm for optimization and uncertainty assessment for hydrologic model parameters. Water Resour. Res. 39(8):1201, doi:10.1029/2002WR001642.

Vrugt J.A., C.J.F. ter Braak, M.P. Clark, J.M. Hyman, B.A. Robinson. 2008. Treatment of input uncertainty in hydrologic modeling: Doing hydrology backward with Markov chain Monte Carlo simulation. Water Resour. Res., 44, W00B09. doi: 10.1029/2007WR006720

Younes A., T.A. Mara, N. Fajraoui, F. Lehmann, B. Belfort, H. Beydoun. 2013. Use of Global Sensitivity Analysis to Help Assess Unsaturated Soil Hydraulic Parameters. Vadose Zone J. 12. doi:10.2136/vzj2011.0150

Hydrol. Earth Syst. Sci. Discuss., doi:10.5194/hess-2016-295, 2016
Manuscript under review for journal Hydrol. Earth Syst. Sci.
Published: 20 June 2016

List of table captions

Table 1. Prior lower and upper bounds of the uncertainty parameters and reference values.

Table 2. Measurement sets and injection periods for the different scenarios. The pressure head h and the water content θ are measured at 5 cm from the top of the column. The cumulative outflow Q and the concentration C are measured at the exit of the column.

Table 3. Summary of the pairwise parameter correlations.

Hydrol. Earth Syst. Sci. Discuss., doi:10.5194/hess-2016-295, 2016
Manuscript under review for journal Hydrol. Earth Syst. Sci.
Published: 20 June 2016

Parameters	**Lower bounds**	**Upper bounds**	**Reference values**
k_s [cm min^{-1}]	0.025	0.1	0.0347
θ_s [-]	0.3	0.5	0.43
θ_r [-]	0.05	0.2	0.09
α [cm^{-1}]	0.01	0.3	0.04
n [-]	1.2	5	1.4
a_l [cm]	0.05	0.6	0.2

Table 1. Prior lower and upper bounds of the uncertainty parameters and reference values.

Scenario	**Measured variables**				**injection period**	
	h	θ	Q	C	$T_{inj} = 5000\,\mathrm{min}$	$T_{inj} = 3000\,\mathrm{min}$
1	ν		ν		ν	
2	ν	ν	ν		ν	
3	ν	ν	ν	ν	ν	
4	ν		ν	ν	ν	
5	ν		ν	ν		ν
6			ν	ν	ν	
7			ν	ν		ν

Table 2. Measurement sets and injection periods for the different scenarios. The pressure head h and the water content θ are measured at 5 cm from the top of the column. The cumulative outflow Q and the concentration C are measured at the exit of the column.

Hydrol. Earth Syst. Sci. Discuss., doi:10.5194/hess-2016-295, 2016
Manuscript under review for journal Hydrol. Earth Syst. Sci.
Published: 20 June 2016

Hydrology and Earth System Sciences
Open Access
Discussions

Scenario					
1	(k_s, n)	(k_s, α)			(θ_r, θ_s)
2	(k_s, n)	(k_s, α)	(k_s, θ_r)	(θ_r, n)	
3	(k_s, n)	(k_s, α)	(k_s, θ_r)	(θ_r, n)	
4	(k_s, n)	(k_s, α)	(k_s, θ_r)	(θ_r, n)	
5	(k_s, n)	(k_s, α)	(k_s, θ_r)	(θ_r, n)	
6	(k_s, n)			(θ_r, n)	
7	(k_s, n)			(θ_r, n)	

Table 3. Summary of the pairwise parameter correlations.

Hydrol. Earth Syst. Sci. Discuss., doi:10.5194/hess-2016-295, 2016
Manuscript under review for journal Hydrol. Earth Syst. Sci.
Published: 20 June 2016

Hydrology and Earth System Sciences
Open Access
Discussions

List of figure captions

Fig. 1. Reference pressure head at 5 cm from the soil surface. Solid lines represent model outputs and dots represent the sets of perturbed data serving as conditioning information for model calibration.

Fig. 2. Reference water content at 5 cm from the soil surface [see Fig. 1 caption].

Fig. 3. Reference cumulative outflow [see Fig. 1 caption].

Fig. 4. Reference retention curve for the infiltration experiment [see Fig. 1 caption].

Fig. 5. Reference breakthrough output concentration for T_{inj} = 5000. [see Fig. 1 caption].

Fig. 6. Reference breakthrough output concentration for T_{inj}= 3000 min. [see Fig. 1 caption].

Fig. 7. MCMC solutions for the transport scenario 1. The diagonal plots represent the inferred posterior probability distribution of the model parameters. The off-diagonal scatterplots represent the pairwise correlations in the MCMC drawing.

Fig. 8. MCMC solutions for transport scenario 2 [see Fig. 7 caption].

Fig. 9. MCMC solutions for transport scenario 3 [see Fig. 7 caption].

Fig. 10. MCMC solutions for transport scenario 4 [see Fig. 7 caption].

Fig. 11. MCMC solutions for transport scenario 5 [see Fig. 7 caption].

Fig. 12. MCMC solutions for transport scenario 6 [see Fig. 7 caption].

Fig. 13. MCMC solutions for transport scenario 7 [see Fig. 7 caption].

Fig. 14. Posterior mean values and 95% confidence intervals of the saturated hydraulic conductivity for the different scenarios.

Fig. 15. Posterior mean values and 95% confidence intervals of the saturated water content for the different scenarios.

Fig. 16. Posterior mean values and 95% confidence intervals of the residual water content for the different scenarios.

Fig. 17. Posterior mean values and 95% confidence intervals of the shape parameter □ for the different scenarios.

Fig. 18. Posterior mean values and 95% confidence intervals of the shape parameter n for the different scenarios.

Fig. 19. Posterior mean values and 95% confidence intervals of dispersivity for the different scenarios.

Hydrol. Earth Syst. Sci. Discuss., doi:10.5194/hess-2016-295, 2016
Manuscript under review for journal Hydrol. Earth Syst. Sci.
Published: 20 June 2016

Hydrology and Earth System Sciences
Open Access
Discussions

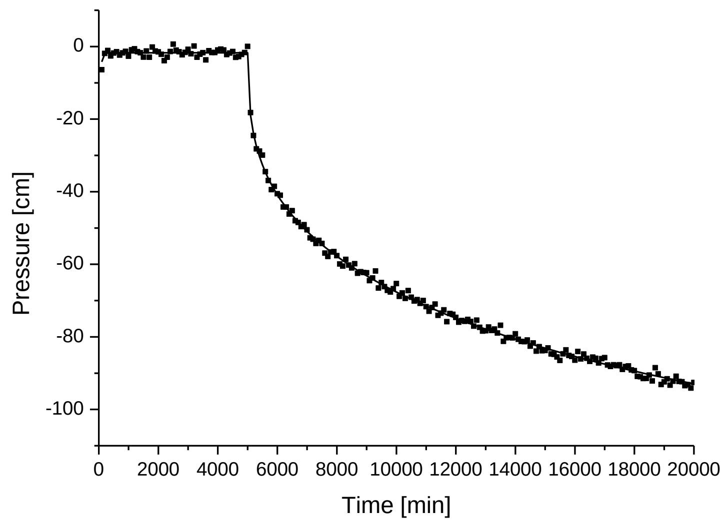

Fig. 1. Reference pressure head at 5 cm from the soil surface. Solid lines represent model outputs and dots represent the sets of perturbed data serving as conditioning information for model calibration.

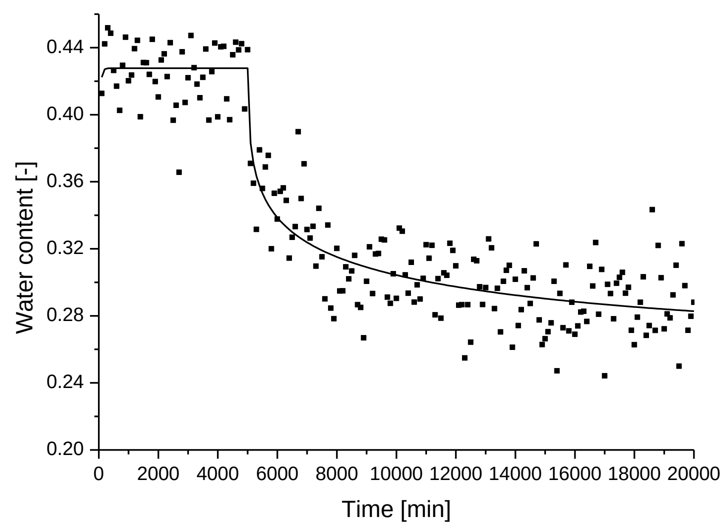

Fig. 2. Reference water content at 5 cm from the soil surface [see Fig. 1 caption].

Hydrol. Earth Syst. Sci. Discuss., doi:10.5194/hess-2016-295, 2016
Manuscript under review for journal Hydrol. Earth Syst. Sci.
Published: 20 June 2016

Hydrology and Earth System Sciences
Open Access
Discussions

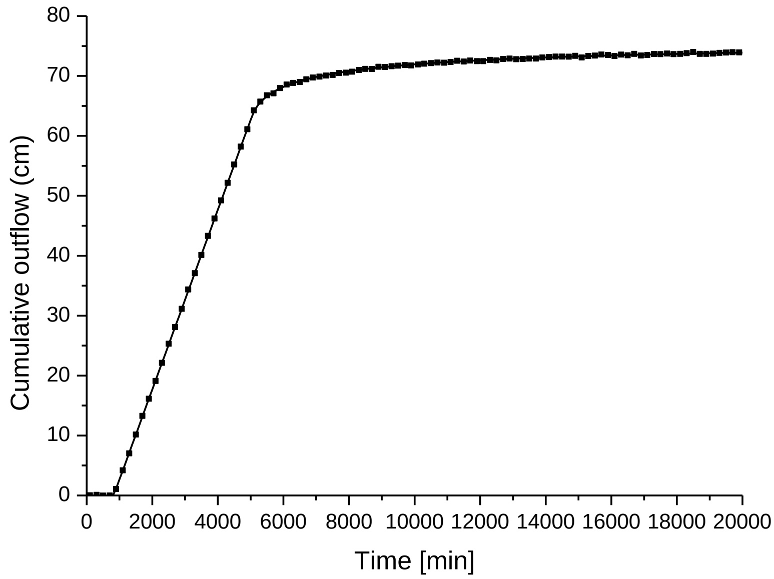

Fig. 3. Reference cumulative outflow [see Fig. 1 caption].

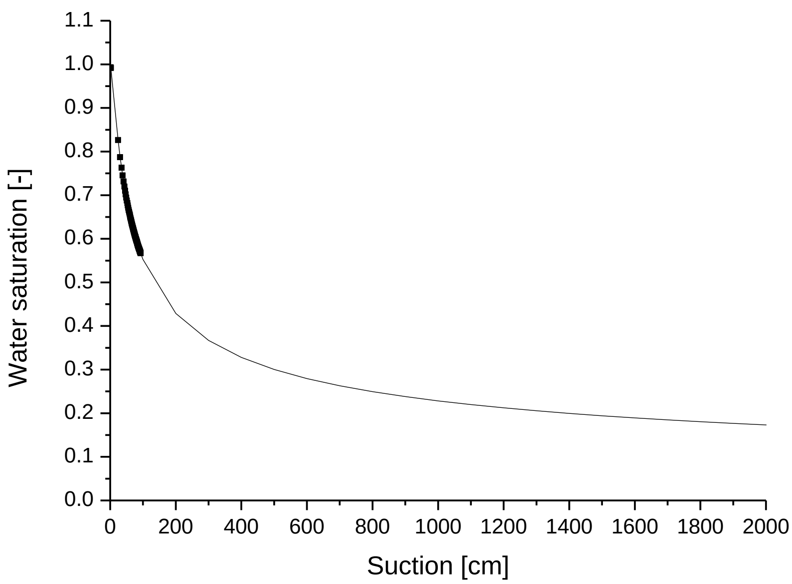

Fig. 4. Reference retention curve for the infiltration experiment [see Fig. 1 caption].

Hydrol. Earth Syst. Sci. Discuss., doi:10.5194/hess-2016-295, 2016
Manuscript under review for journal Hydrol. Earth Syst. Sci.
Published: 20 June 2016

Hydrology and Earth System Sciences
Open Access
Discussions

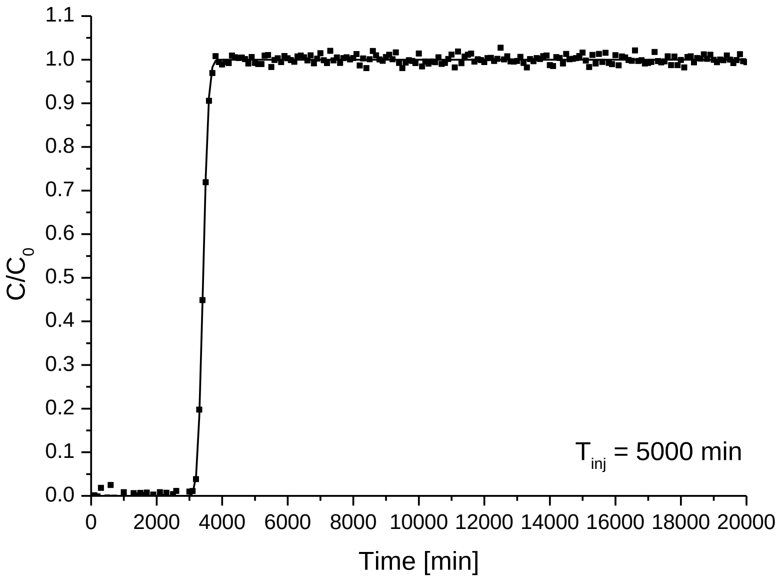

Fig. 5. Reference breakthrough output concentration for T_{inj} = 5000. [see Fig. 1 caption].

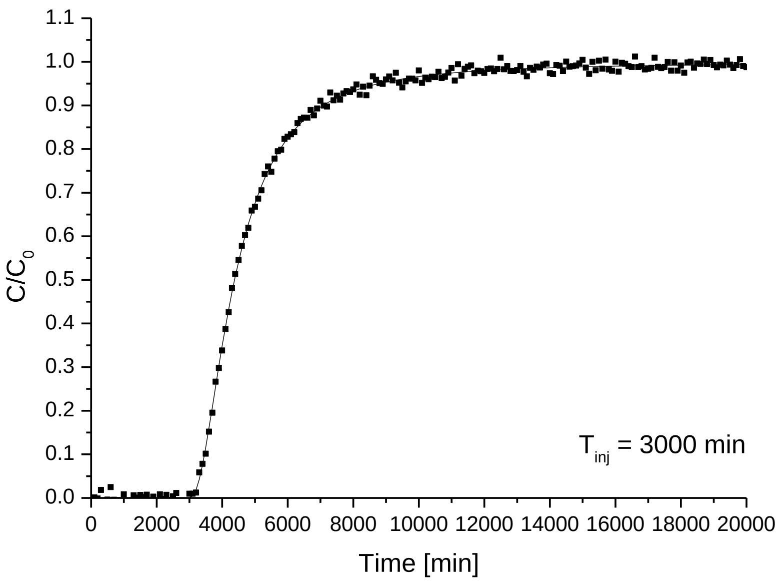

Fig. 6. Reference breakthrough output concentration for T_{inj}= 3000 min. [see Fig. 1 caption].

Hydrol. Earth Syst. Sci. Discuss., doi:10.5194/hess-2016-295, 2016
Manuscript under review for journal Hydrol. Earth Syst. Sci.
Published: 20 June 2016

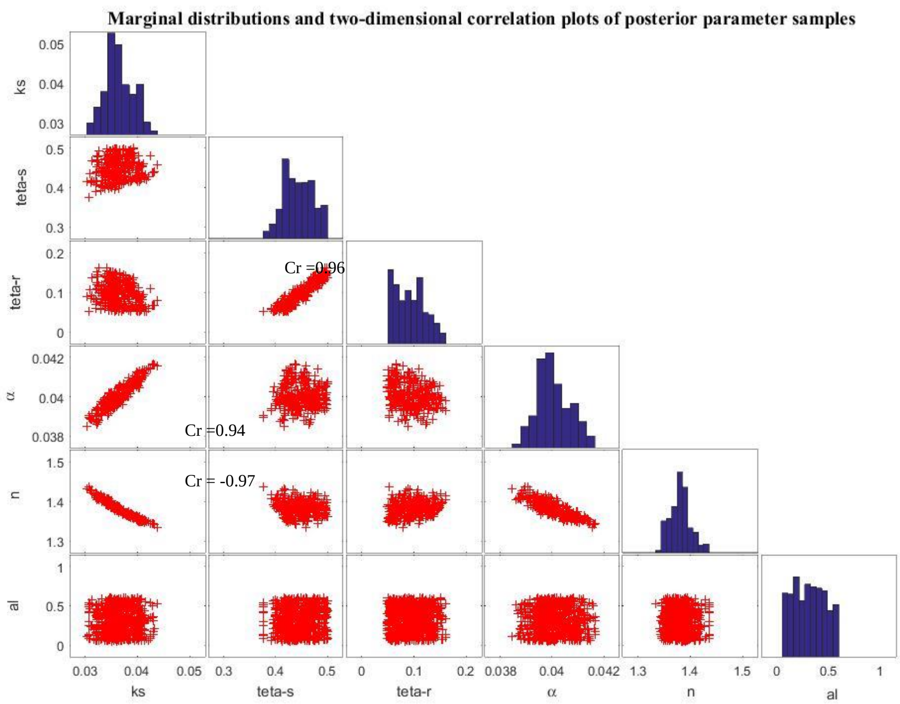

Fig. 7. MCMC solutions for the transport scenario 1. The diagonal plots represent the inferred posterior probability distribution of the model parameters. The off-diagonal scatterplots represent the pairwise correlations in the MCMC drawing.

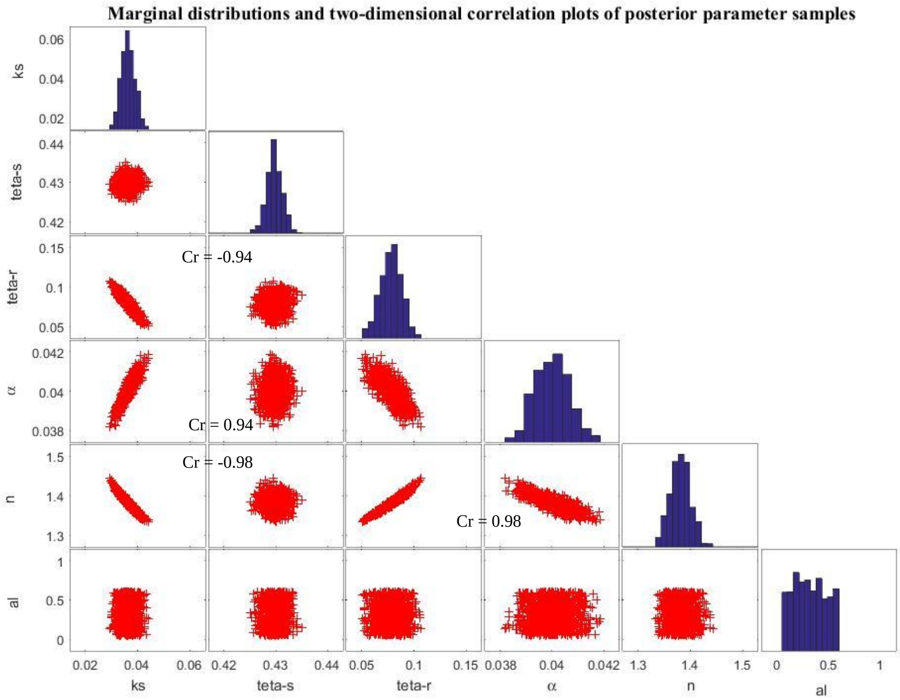

Fig. 8. MCMC solutions for transport scenario 2 [see Fig. 7 caption].

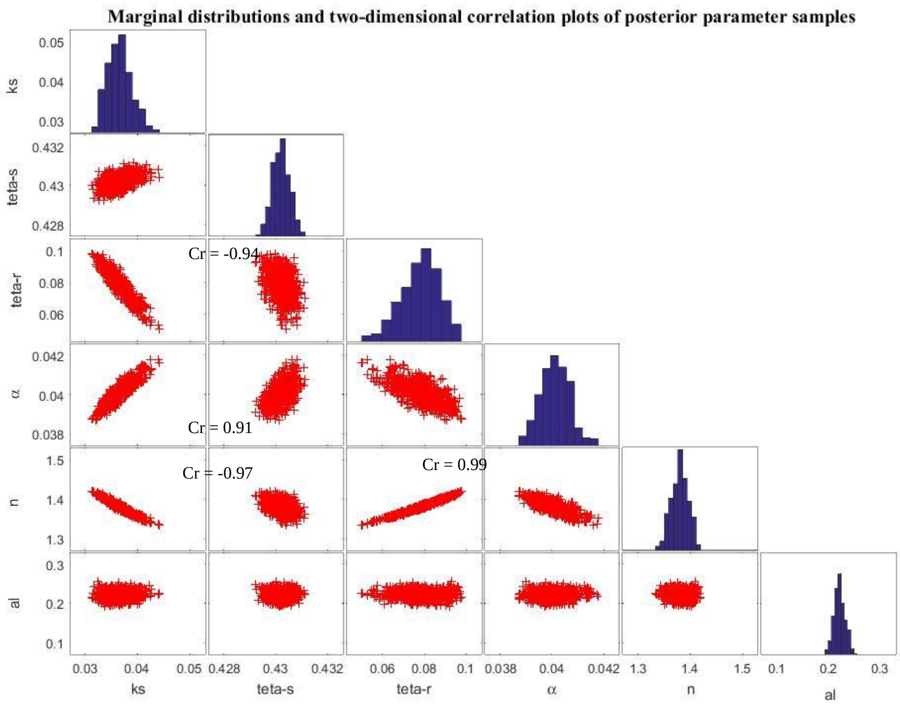

1
2 Fig. 9. MCMC solutions for transport scenario 3 [see Fig. 7 caption].

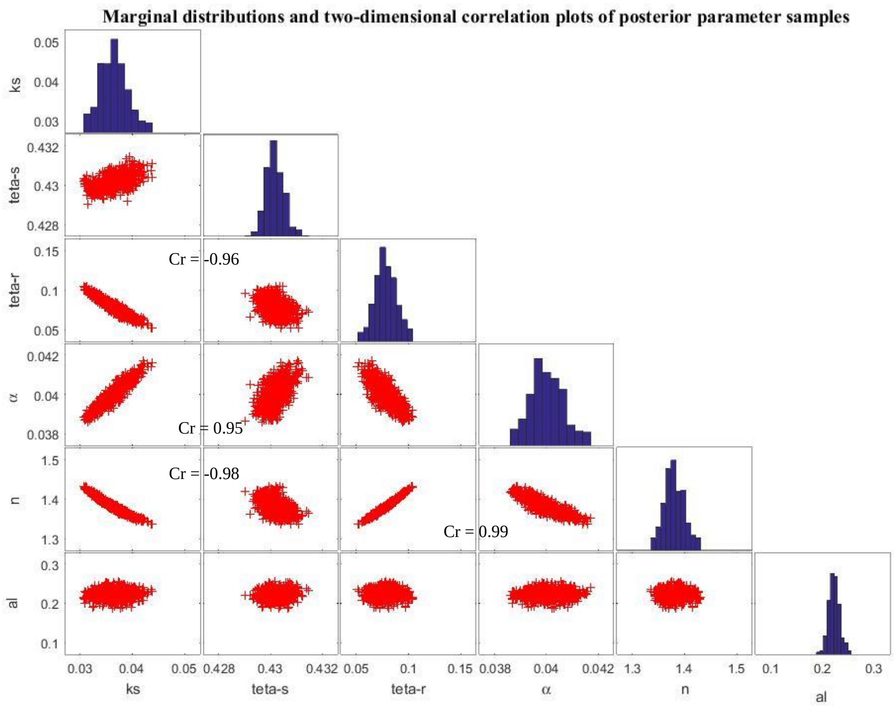

Fig. 10. MCMC solutions for transport scenario 4 [see Fig. 7 caption].

Hydrol. Earth Syst. Sci. Discuss., doi:10.5194/hess-2016-295, 2016
Manuscript under review for journal Hydrol. Earth Syst. Sci.
Published: 20 June 2016

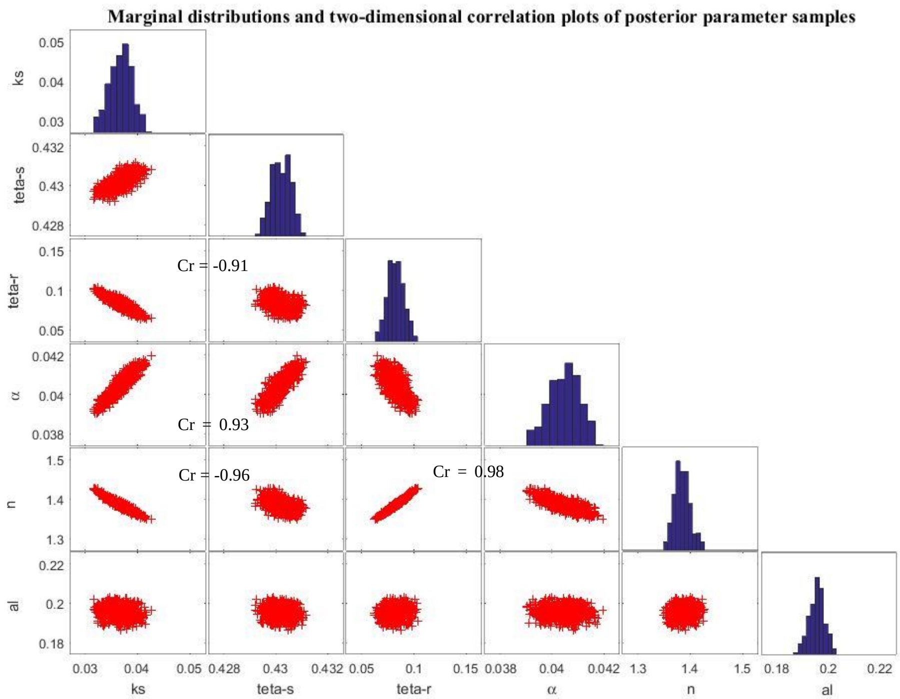

1
2 Fig. 11. MCMC solutions for transport scenario 5 [see Fig. 7 caption].

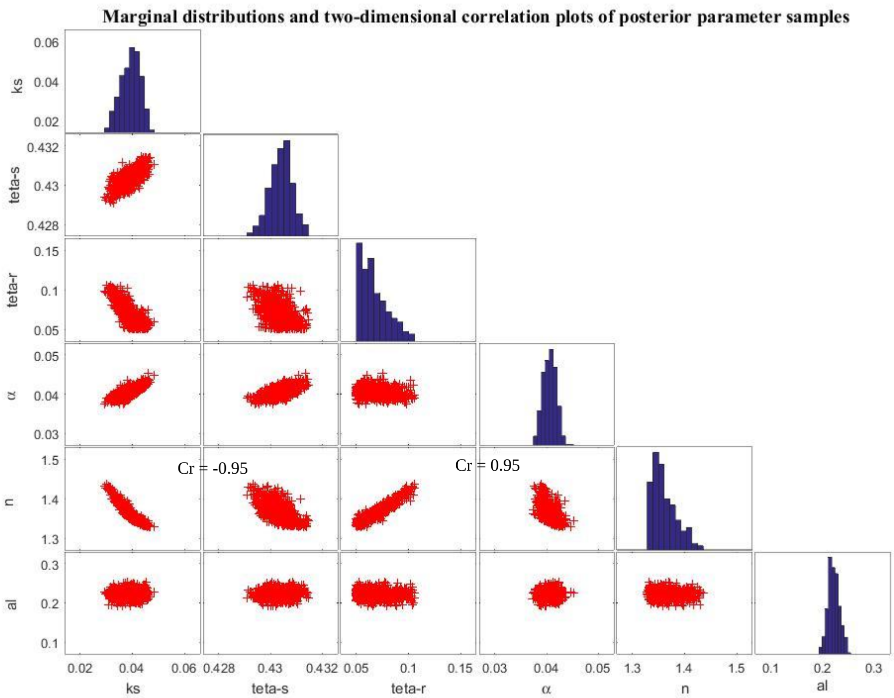

Fig. 12. MCMC solutions for transport scenario 6 [see Fig. 7 caption].

Hydrol. Earth Syst. Sci. Discuss., doi:10.5194/hess-2016-295, 2016
Manuscript under review for journal Hydrol. Earth Syst. Sci.
Published: 20 June 2016

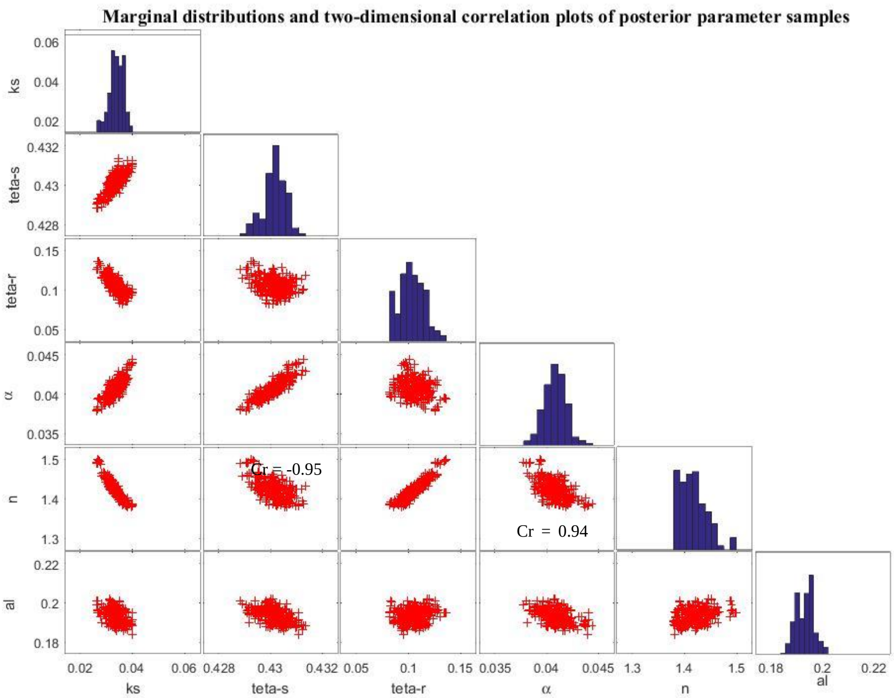

1
2 Fig. 13. MCMC solutions for transport scenario 7 [see Fig. 7 caption].

Hydrol. Earth Syst. Sci. Discuss., doi:10.5194/hess-2016-295, 2016
Manuscript under review for journal Hydrol. Earth Syst. Sci.
Published: 20 June 2016

Hydrology and Earth System Sciences
Open Access
Discussions

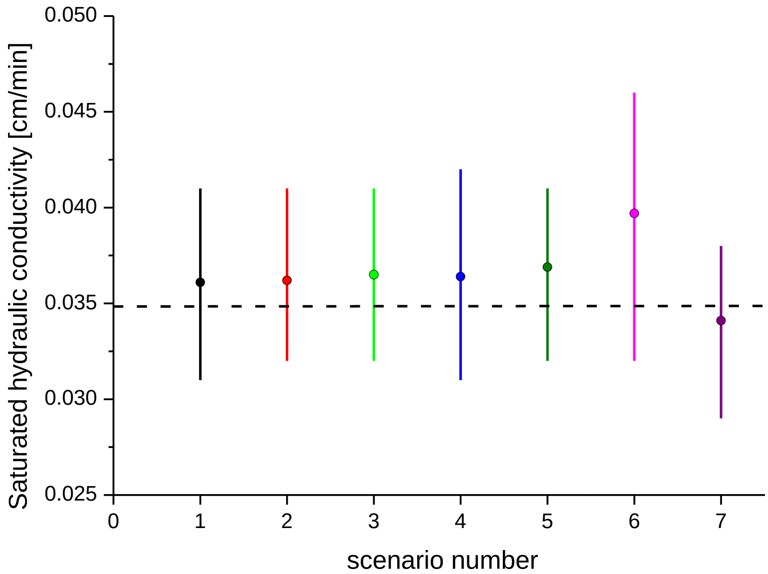

Fig. 14. Posterior mean values and 95% confidence intervals of the saturated hydraulic conductivity for the different scenarios.

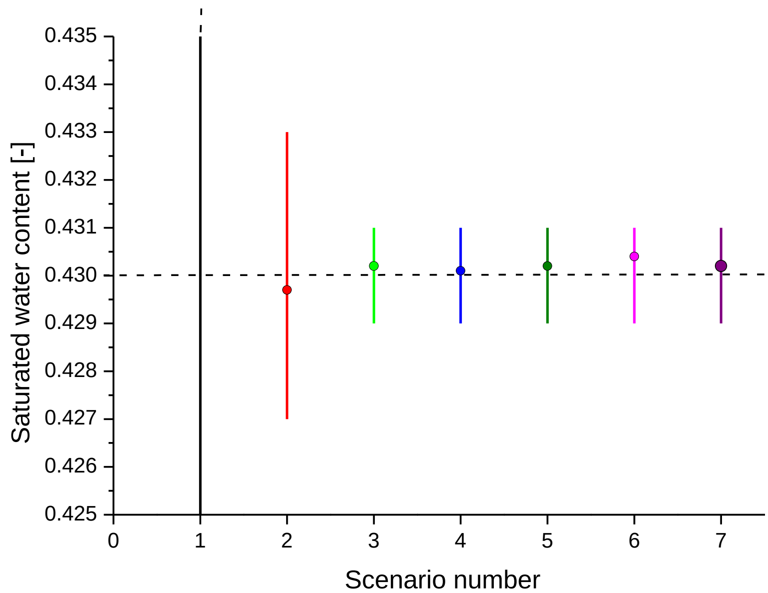

Fig. 15. Posterior mean values and 95% confidence intervals of the saturated water content for the different scenarios.

Hydrol. Earth Syst. Sci. Discuss., doi:10.5194/hess-2016-295, 2016
Manuscript under review for journal Hydrol. Earth Syst. Sci.
Published: 20 June 2016

Hydrology and Earth System Sciences
Discussions
Open Access

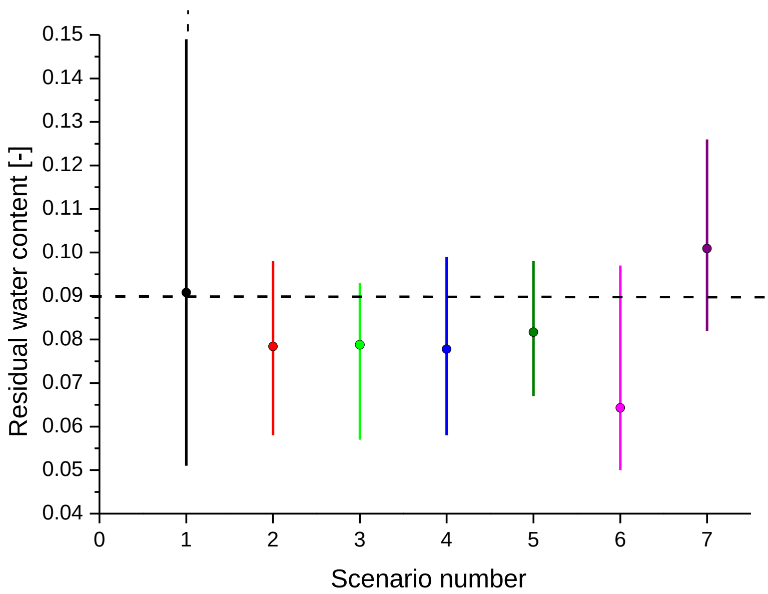

Fig. 16. Posterior mean values and 95% confidence intervals of the residual water content for the different scenarios.

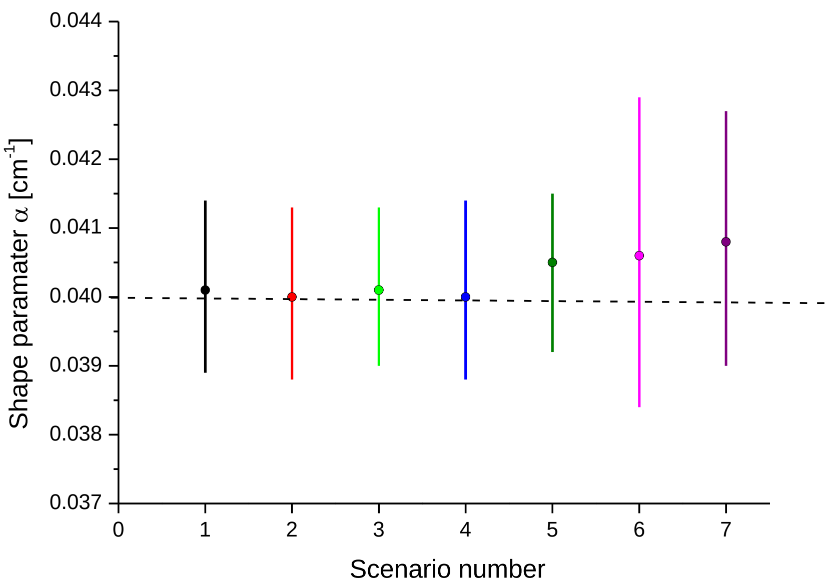

Fig. 17. Posterior mean values and 95% confidence intervals of the shape parameter for the different scenarios.

Hydrol. Earth Syst. Sci. Discuss., doi:10.5194/hess-2016-295, 2016
Manuscript under review for journal Hydrol. Earth Syst. Sci.
Published: 20 June 2016

Hydrology and Earth System Sciences
Discussions

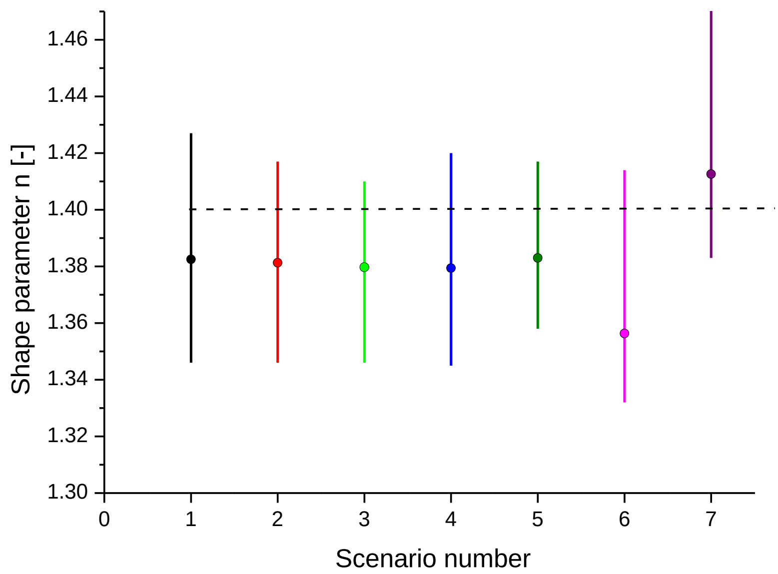

Fig. 18. Posterior mean values and 95% confidence intervals of the shape parameter n for the different scenarios.

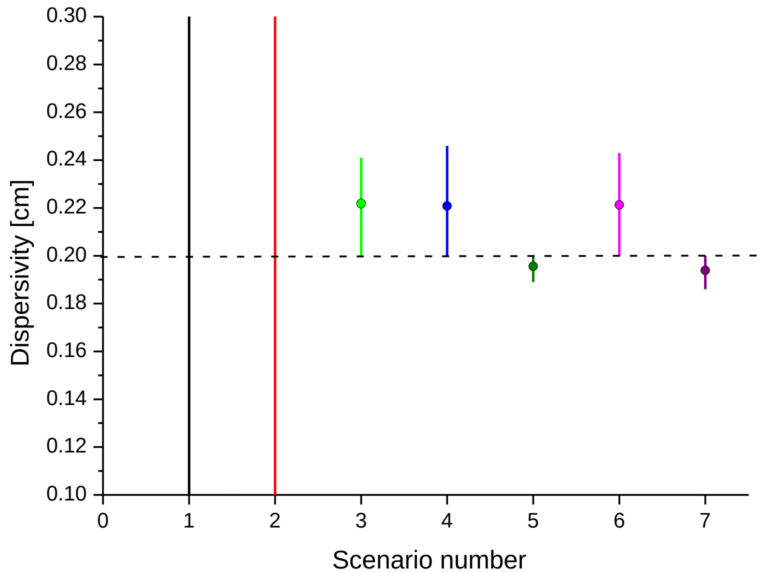

Fig. 19. Posterior mean values and 95% confidence intervals of dispersivity for the different scenarios.